Journal of Manufacturing Processes 30 (2017) 431–438

Contents lists available at ScienceDirect

Journal of Manufacturing Processes

journal homepage: www.elsevier.com/locate/manpro

Research paper

Electric field manipulation for deposition control in near-field electrospinning

Xiangyu You, Chengcong Ye, Ping Guo*

Department of Mechanical and Automation Engineering, The Chinese University of Hong Kong, Shatin, N.T., Hong Kong Special Administrative Region

ARTICLE INFO

Article history:
Received 1 June 2017
Received in revised form 14 August 2017
Accepted 5 October 2017
Available online 17 October 2017

Keywords:
Near-field electrospinning
Electric field manipulation
Deposition control

ABSTRACT

Electrospinning is recognized as an efficient and versatile technique that has been widely used in nanoscale fiber fabrication. Electric field manipulation is one of the efficient ways to precisely control an electrospinning jet. While there have been several studies of the electric field manipulation effect on nanofiber deposition control, these works are limited to the control of a far-field electrospinning (FFES) jet to deposit in one dimension or to suppress the chaotic whipping mode to some extent. Few work has been done to control a near-field electrospinning (NFES) jet for deposition of complex patterns using electric field manipulation. To this end, we propose a novel design by adding a moving sharp-pin electrode beneath the plane collector. The sharp pin electrode is charged with a positive voltage and moved to redistribute the electric field for jet trajectory control, while the plane collector is kept stationary. The focusing of the electric field and the guiding effect of the jet trajectory due to the additional sharp-pin electrode are studied and demonstrated. Various parameters (voltage, electrode translation speed, and collection mechanism) are analyzed to experimentally study their effects on the fiber deposition control. It is demonstrated in the current work the feasibility of controlling a single fiber for deposition of complex patterns in near-field electrospinning by manipulating the electric field distribution.

1. Introduction

Electrospinning, one of the most efficient techniques for fabricating nanofibers, has attracted considerable attention from researchers due to its cost-effectiveness and versatility. Due to their numerous advantages such as large surface-to-volume ratio, high flexibility, small diameter and porosity, electrospun nanofibers have been used in various applications including metal recovery filters [1], biologically protective clothing [2], wound dressings [3], drug delivery [4,5], energy harvesters [6], sensors and actuators [7,8], etc.

The fundamental idea of electrospinning dates to 1930s [9], when a series of patents [9–11] were published to describe the experimental setup for the production of polymer fibers using electrostatic force. A typical electrospinning setup is schematically shown in Fig. 1. In an electrospinning process, a polymer solution or melt polymer is dispensed through a syringe pump, causing the formation of a droplet at the tip of the spinneret. When a voltage is applied, the electrostatic force makes the meniscus of droplet deform into a conical shape which is called a Taylor cone. To overcome the surface tension, a high voltage (typically on the order of 10^5 V/m [12]) is used to create a polymer jet initiated from the Taylor cone. The solvent or melt polymer is usually positively charged and the collector is grounded. Before reaching the collecting screen, the electrically charged jet solidifies or evaporates; it is then collected as fibers on the collector [13]. However, the registry of fibers on the collector is typically random due to the bending instability, which is caused by repulsive forces originated from the charged elements within an electrospinning jet [14]. The disorder of deposited fibers has limited its full process potential. Electric field manipulation is one of the efficient ways to precisely control an electrospinning jet. Several works have been done to control the deposition of nanofibers using electric field manipulation. Li et al. [15] used a collector composed of two conductive strips separated by an insulating gap to generate uniaxially aligned nanofiber arrays. Carnell et al. [16] demonstrated highly aligned electrospun nanoscale fibers in one dimension produced via electrospinning by incorporating an auxiliary counter electrode to create an electric field with controlled distribution and magnitudes. Deitzel et al. [13] studied the feasibility of dampening the chaotic instability and controlling the fiber deposition by using an electrostatic lens element. Lee et al. [17] used a sharp-pin ground electrode and a cylindrical side-wall electrode to focus the electrospinning jet for the fabrication of various patterned thick mats and nanofibrous patterns.

* Corresponding author.
E-mail addresses: pguo@mae.cuhk.edu.hk, steven.guoping@gmail.com (P. Guo).

https://doi.org/10.1016/j.jmapro.2017.10.005
1526-6125/

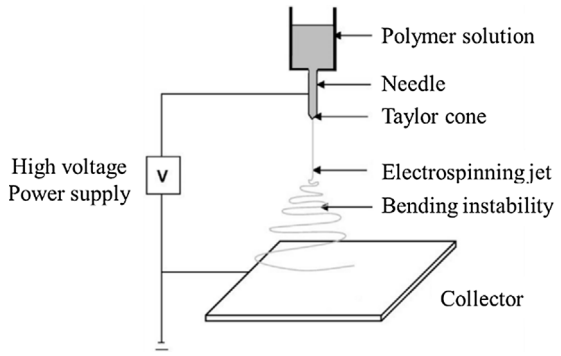

Fig. 1. Schematic of the electrospinning process.

However, these works are limited to the control of far-field electrospinning (FFES) jet to deposit in one dimension or to suppress the chaotic whipping mode to some extent. The precise control of a single electrospinning fiber for complex patterns is still a challenging task.

Near-field electrospinning (NFES) is a novel way to deposit solid nanofibers with orderly patterns. Sun et al. [18] demonstrated the setup of a NFES process, which was capable of depositing nanofibers in a direct, continuous, and controllable manner. The main difference of the configurations between NFES and FFES is the nozzle-to-collector distance and the applied voltage. The nozzle-to-collector distance is reduced significantly from several centimeters to few millimeters to reduce the bending instability. The applied voltage is substantially lowered to several hundred volts due to the reduced distance. Some encouraging initial results were produced to demonstrate the possibility of achieving complex patterns of nanofibers taking advantage of NFES. Hellmann et al. [19] reported the "House of Santa Claus" motif written by PAN nanofibers. Chang et al. [20] demonstrated the fabricated three-character "Cal" on a silicon chip using a programmable XY stage. Bisht et al. [21] developed a computer-controlled setup for NFES to improve the process performance and reliability. They demonstrated the fabrication of straight continuous fiber patterns using the proposed setup. Wei and Dong [22] demonstrated high-resolution printing of 2D and 3D fiber structures using electrohydrodynamic hot jet plotting with an extremely small nozzle-substrate gap at 170 μm. Brown et al. [23] reported the direct writing of 3D scaffolds by way of melt near-field electrospinning. NFFS is an efficient way to precisely control the electrospinning jet which can suppress the bending instabilities dramatically and make the process more stable. Nevertheless, no work has been done to control a NFES jet for complex pattern deposition purely depending on the manipulation of the electric field distribution.

In this work, a novel design by adding a moving sharp-pin electrode beneath a stationary collector is proposed to control a melt electrospinning jet for deposition of complex patterns by utilizing only the distribution of the electric field. The focusing of the electric field and the guiding effect of the jet trajectory due to the additional sharp-pin electrode are studied and demonstrated. Various parameters (voltage, translation speed, and collection mechanism) are analyzed to experimentally study their effects on the fiber deposition control.

2. Experimental setup

Poly (ε-caprolactone) (PCL) with a molecular weight of 80,000 g/mol and a melting point of 60 °C was selected as the fiber material for its excellent electrospinning characteristics (good biological property and high thermal stability). The experimental configuration based on near-field melt electrospinning is shown in Fig. 2. The PCL beads were loaded into a 1.5 mL stainless steel syringe fitted with a needle of gauge 26. The needle acted as the dispensing nozzle, which has an inner diameter of 0.26 mm and a length of 10 mm. A proportional-integral-derivative (PID) regulated electrical heating system was adopted to keep the molten polymer at a stable temperature at 90 °C. A precision syringe pump (Harvard Apparatus, Remote Infuse/Withdraw PHD Ultra Syringe Pump) was used to dispense the polymer solution at a feed rate of 10 μL/h.

The nozzle-to-collector distance was maintained at 2 mm and the collector was kept stationary. A movable sharp-pin electrode was installed beneath the polyethylene film collector. The distance between the pin and the collector was 100 μm. In the experiment, the bottom pin electrode was positively charged and the nozzle was grounded. The collector, which is a dielectric material, was isolated in the electric field. Special care has been made to ensure the collector was not grounded (otherwise the electrospinning process would not be initiated). The polarization of the collector produced an electric field opposing to the applied electric field, which would reduce the effective electric field strength. The reduction amount was determined by the material relative permittivity and thickness. So, we selected a material with low relative permittivity (2.25) and small thickness (100 μm), polyethylene, as the collector material.

The sharp-pin electrode was mounted on a programmable X-Y-Z stage (Aerotech Inc.). The resolution in the X-, Y- and Z- axes is 1 nm respectively. The maximal velocity in each axis is 350 mm/s. The stage is controlled by an A3200 software-based machine controller (Aerotech Inc.) with the motion capabilities including point-to-point, linear, circular, helical, and spherical interpolations. A microscopic camera (Point Grey Research) was used to monitor and record the electrospinning process. The whole setup was stationed on a granite table. The experiment was carried out at room temperature and atmospheric pressure. The initial polymer jet was self-initiated by applying a high voltage at a predefined value. The electrostatic force would first deform the meniscus of droplet into a Taylor cone. Then the surface tension would be overcome by the electrostatic force with the accumulation of the electrostatic charges, causing a polymer jet initiated from the Taylor cone to start the electrospinning process. The whole initiation process is shown in Fig. 3.

3. Results and discussions

3.1. Electric field focusing and jet trajectory guiding

A convergent electric field is preferred in near-field melt electrospinning to reduce the whipping motion and to stabilize the jet trajectory. To satisfy this demand, a pin-to-pin configuration is proposed to focus and to control the distribution of the electric field as shown in Fig. 2(a). There are three major differences between a conventional near-field electrospinning setup and our proposed design. (1) A bottom pin electrode is used to replace the plane collector electrode in a conventional process. It is used to create a convergent electric field for jet trajectory guiding. (2) The bottom pin electrode is charged with a positive voltage while the spinneret is grounded, which eliminates the interference from the surrounding grounded objects. (3) The plane collector is kept stationary, while the pin electrode is moved to guide the fiber trajectory. The electrospinning jet would be attracted by the pin electrode, and follow the trajectory of the pin electrode. Finite element analysis was used to simulate the electric field distribution of the conventional electrode design with a conductive plate and the proposed design with a sharp-pin electrode to demonstrate the effects of electric field focusing and electrospinning jet guiding.

We modeled and simulated the electric field in 2D space using the COMSOL Multiphysics software. In the model, the nozzle to

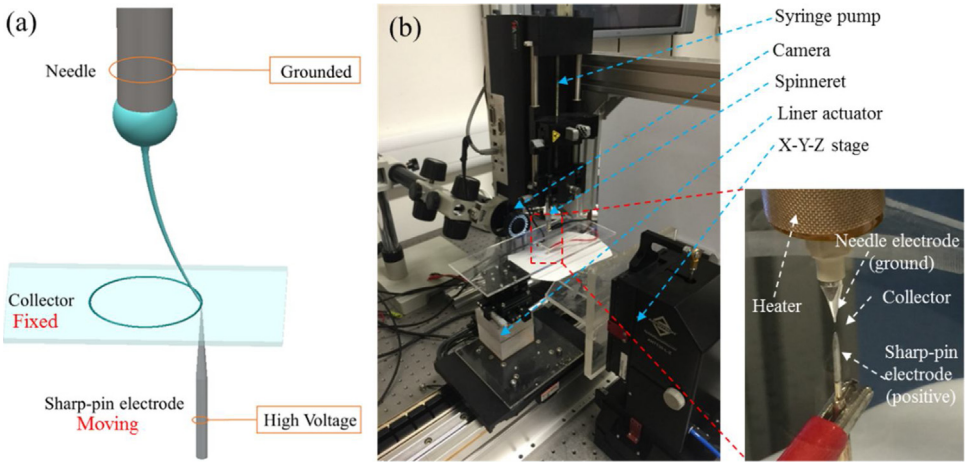

Fig. 2. (a) Schematic of the proposed electrospinning apparatus; and (b) actual experimental setup.

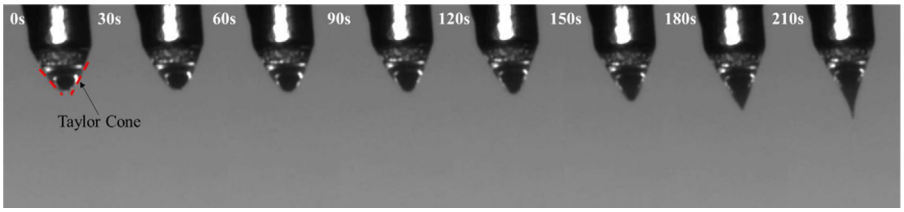

Fig. 3. The jet initiation process for near-field melt electrospinning.

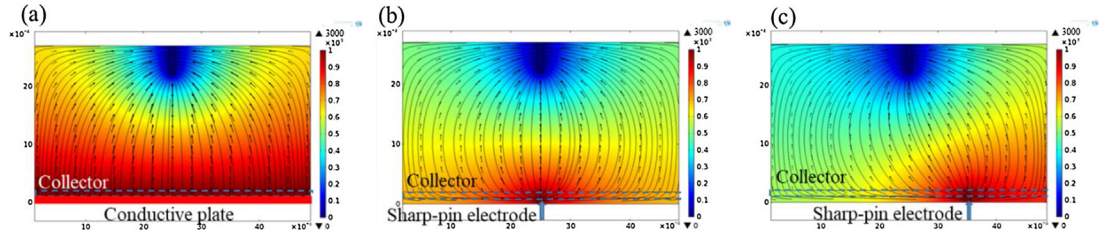

Fig. 4. Electric field simulation results for (a) a conventional plane bottom electrode and a sharp-pin bottom electrode configuration (b) without an offset and (c) with an offset of 1 mm.

collector distance was 2 mm, the applied voltage on the electrode beneath the collector was 3000 V and the nozzle was grounded. The medium between the printing nozzle and the collector was set as air with relative permittivity 1. The material properties of the collector were set according to the experimental conditions (relative permittivity of 2.25 and thickness of 100 μm). The simulation results of electric field lines were plotted in Fig. 4 for three different electrode configurations. As seen in Fig. 4(a), electric field lines in the conventional electrode design were nearly uniformly distributed close to the collector plane, which indicated that the attraction force was not convergent. While in Fig. 4(b), electric field lines in the proposed sharp-pin electrode design were directed towards the pin electrode, indicating that the attraction force was converged to the pin electrode. In Fig. 4(c), the pin electrode was shifted with an offset of 1 mm. The simulation results showed that the electric field lines converged towards the pin electrode with the same offset. It indicated that the electric force acting on the electrospinning jet would guide the jet towards the pin electrode.

As shown in Fig. 4, at the region close to the collector. The electric field lines were not only convergent to the bottom pin electrode, but also had lateral components pointing to the intended jet trajectory (the straight line connecting the nozzle and the bottom pin). These concentric lateral components help to exert a force that will reduce the whipping motion to some extent [16,24,25]. It should be noted, at the region near the nozzle, the electric field was divergent. The whipping motion, however, has not been established at the close near-field, where the jet motion was dominated by its initial ejecting velocity.

From the simulation results, the proposed pin electrode design would have a better focusing and stabilization effect on the electrospinning jet compared with the conventional plane electrode setup. In addition, it was demonstrated that it would be possible to use a moving bottom sharp-pin electrode to guide the electrospinning jet trajectory by redistributing the electric field.

The trajectory of an electrospinning jet following the motion of the sharp-pin electrode was monitored and recorded by a microscopic camera, as depicted in Fig. 5. The nozzle-to-collector distance was 2 mm. The applied voltage was 3000 V, while the translation speed of the electrode was 8 mm/s. It was observed that the electrospinning jet followed and attached to the sharp-pin electrode beneath the stationary collector when the sharp-pin electrode was moving from left to right at 8 mm/s, which verified the feasibility of using an electric field to guide the jet trajectory in near-field melt electrospinning.

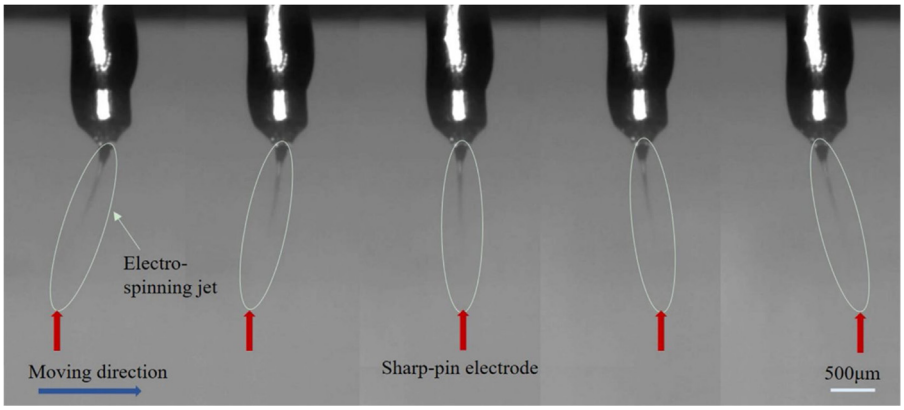

Fig. 5. Trajectory of the electrospinning jet following the motion of a sharp-pin electrode.

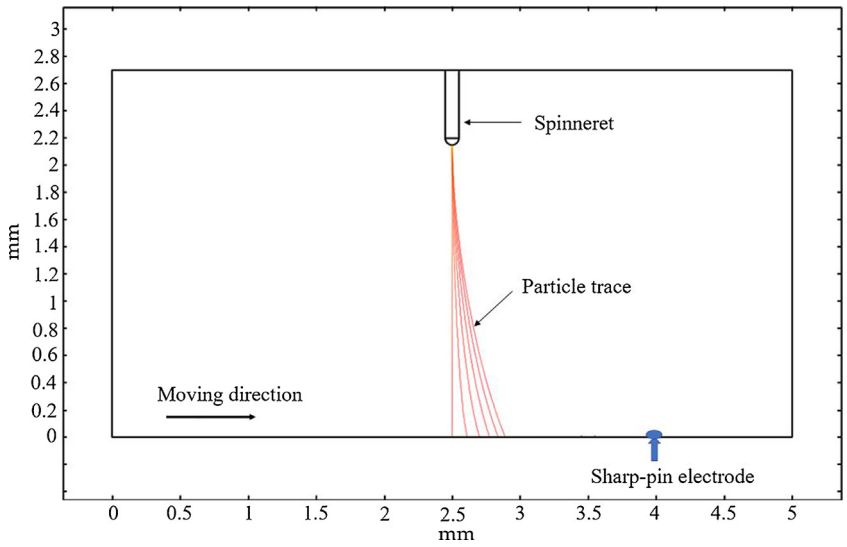

Fig. 6. The simulated trajectories of a charged particle under different offsets of a bottom pin electrode.

3.2. *Influence of voltage on the effective control region*

The sharp-pin electrode can move around to control the trajectory of the electrospinning jet. There, however, exists a control region within which the jet will follow the moving pin electrode. It is attributed to the fact that the shortest path of electric field lines (which indicates the jet trajectory) will only point to the pin electrode if it is within a certain offset range. The simulation results are shown in Fig. 6, where the trajectories of a charged particle subject to different pin electrode offset values. As an example shown in Fig. 6, though the particle trace bends towards right, it does not reach the location of the pin electrode at the collector plane when the pin electrode is offset by 1.5 mm to the center. The effective control region with a shifted bottom pin electrode needs to be further analyzed under different applied voltage.

To study the influence of applied voltage on the effective control region, the pin electrode was moved in a circular pattern with a gradually increased radius up to 1 mm. The nozzle-to-collector distance and the bottom electrode translation speed were 2 mm and 8 mm/s, respectively. The applied voltage was set ranging from 2000 V to 3500 V with a step size of 500 V. The corresponding collected fiber patterns are shown accordingly from Fig. 7(a) to (d). An SEM image of the collected fibers is shown in Fig. 7(e). The measured diameter of collected PCL fibers was 6.80 μm. When the voltage changed from 2000 V to 3500 V, the diameter of the effective control region increased from 952 μm to 1540 μm. A linear relationship between the applied voltage and diameter of the control region was found as plotted in Fig. 7(f).

In Fig. 7(d), wavy patterns are observed due to the buckling effect, which are not presented in Fig. 7(a)–(c). This can be explained by two contributing factors. Firstly, the increased applied voltage resulted in a larger initial jet velocity, making it easier for buckling at the same collection speed. Secondly, with a larger trajectory diameter, the length of the electrospinning jet in the air became longer, which also contributed to the buckling effect. By increasing the plotting speed, the buckling effect can be eliminated. When the pin electrode moved out of the effective control region, the electrospinning jet would no longer follow and attach to the moving pin electrode. The fibers would be randomly collected. When the pin electrode moved further away from the center, the electrospinning process would be interrupted due to the insufficient electric field strength.

3.3. *Influence of lateral translation speed of the bottom electrode on fiber deposition control*

The translation speed of the bottom electrode is another important parameter that can affect the fiber deposition control. Fabricated circular fiber patterns with different electrode translation speeds are shown in Fig. 8. In this part, the pin electrode moved in circular patterns with a fixed radius of 0.3 mm. The nozzle-to-collector distance and applied voltage were kept at 2 mm and

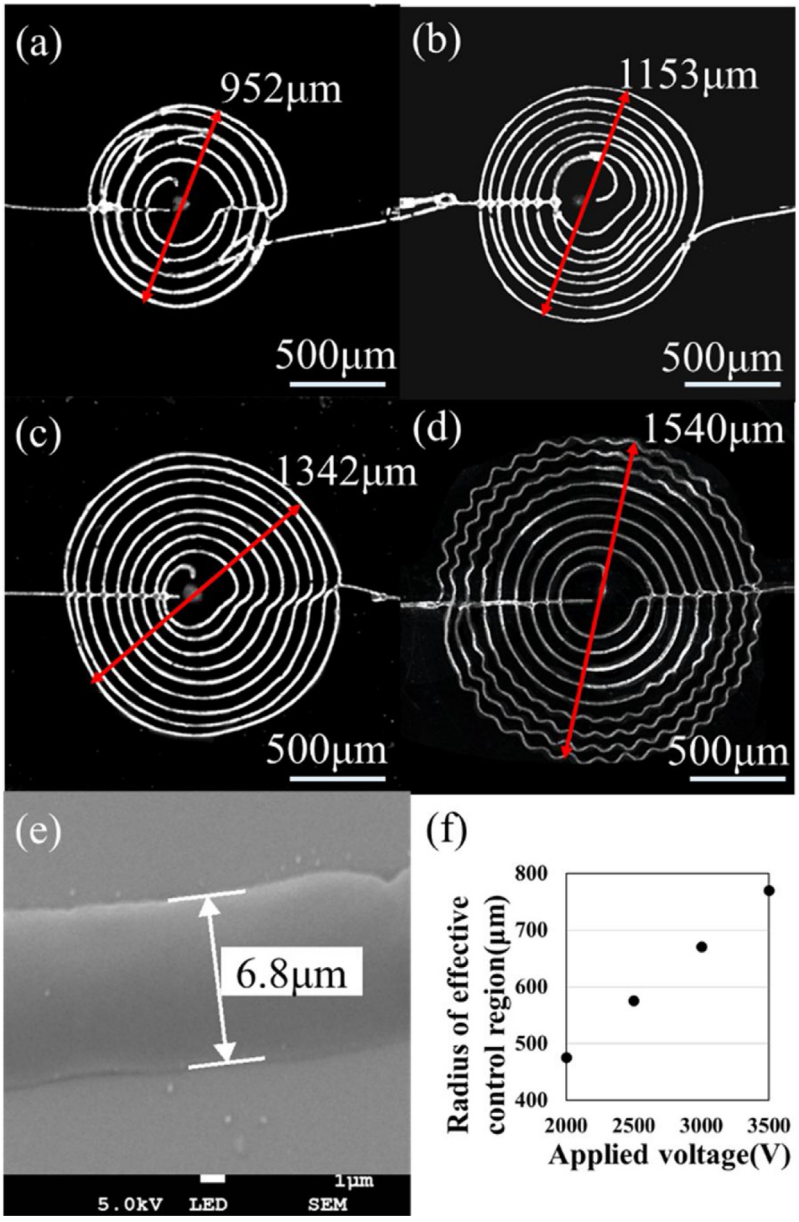

Fig. 7. Effective control region with applied voltage of (a) 2000 V, (b) 2500 V, (c) 3000 V, and (d) 3500 V; (e) SEM image of the collected single fiber; and (f) relationship between the applied voltage and the effective control region.

3000 V, respectively. The translation speed of the pin electrode was varied from 1 mm/s to 9 mm/s with an increment of 1 mm/s corresponding to the results of Fig. 8(a)–(i). It has been observed that the general trend of a circular shape is obtained from all nine cases following the trajectory of the moving pin electrode. However, with a slower translation speed, pronounced waving patterns were formed along the circular trajectory as shown in Fig. 8(a). This was due to the presence of longitudinal compressive force acting on the electrospinning jet, which caused the collected fibers to diverge away from the deposition point directly above the pin electrode with coiling or waving phenomena. With a higher translation speed, the drag force between the bottom electrode and the electrospinning jet would introduce axial tensile force to the jet and reduce the net compressive force. When the translation speed of the bottom electrode was set to a critical value, the increased tensile force would balance the compressive force to eliminate the buckling effect. So, to reduce the waving effect of deposited fibers, the translation speed was increased as shown from Fig. 8(b) to (g). A smooth single fiber circular pattern was obtained with a translation speed of 8 mm/s shown in Fig. 8(h), at which the electrode translation speed reached the critical value. When the electrode translation speed was greater than the critical velocity, the intended circular pattern was distorted as shown in Fig. 8(i). This is due to the fact that the response time would not be enough for the electrospinning jet to precisely follow the change of the electric field, which caused the distortion of the intended trajectory. The critical translation speed depends on the initial jet velocity as well as the length of the electrospinning jet. The translation speed of the bottom electrode should be set as close as possible to this critical velocity to obtain a smooth curved pattern.

3.4. Influence of collection mechanism on fiber deposition control

Traditionally, complex fiber patterns with curved geometry and small feature size are difficult to be deposited using a conventional near-field electrospinning setup. The proposed setup with a mov-

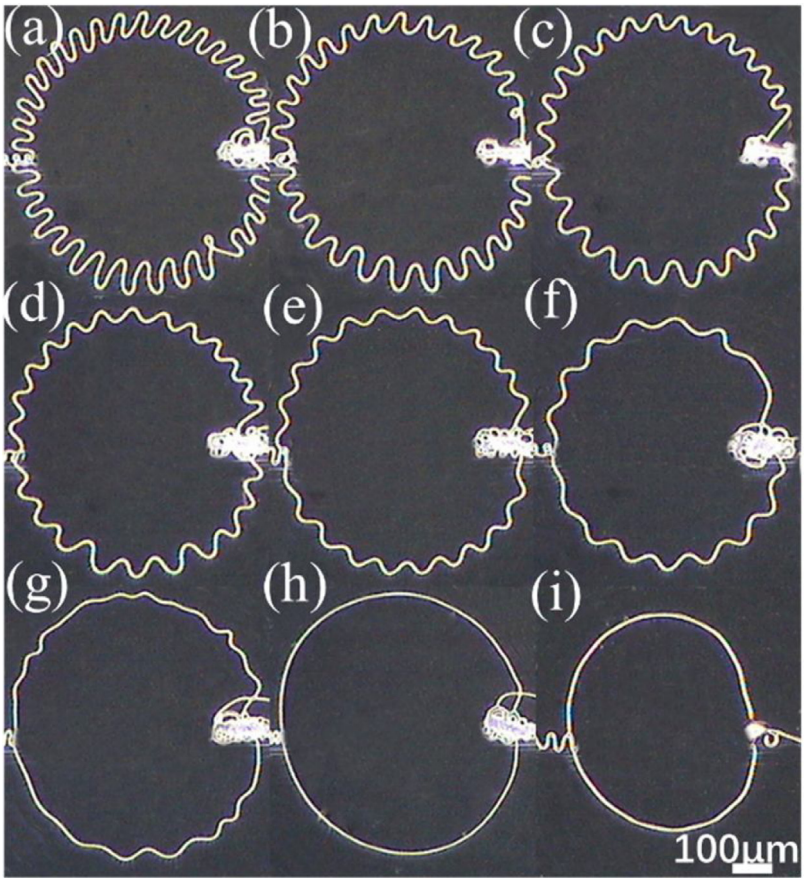

Fig. 8. Fabricated circular fiber patterns with different electrode translation speeds from (a–i) 1 mm/s to 9 mm/s with an increment of 1 mm/s.

able bottom pin electrode and a stationary collector provides an alternative option for better control of the jet trajectory and deposition accuracy. In addition, we have demonstrated the feasibility of controlling an electrospinning jet purely depending on electric field manipulation. By demonstrating the fabrication of complex fiber patterns, the results have shown that the fiber deposition can be effectively controlled utilizing the electric field distribution rather than the mechanical motion of a collector. It is possible in the future work to totally replace the mechanical stage by an electric field manipulation device which will make the whole setup stationary during the NFES process.

In this section, the collection mechanism of two different setups (conventional and proposed ones) are compared and discussed to demonstrate the advantages of the proposed method for better fiber deposition control. In a conventional setup with a movable plane electrode/collector, a delayed zone exists between the desired and actual deposition positions as shown in Fig. 9(a). It is caused by the strong drag force acting on the electrospinning jet from the moving collector, which bends the straight electrospinning jet to a curved trajectory and deteriorates the deposition accuracy. This delay would not be a big problem for deposition of one-dimensional straight line patterns. When two-dimensional curved patterns are deposited, the electrospinning jet, however, could not precisely follow the intended trajectory. The electrospinning jet would not respond to the direction change of the trajectory instantly due to the delayed zone, which causes the distortion of the collected fiber patterns. It is thus hard to fabricate complex two-dimensional patterns using the conventional setup. In our proposed setup, the collector is kept stationary while a bottom pin electrode is utilized to control the electric field distribution. The electrospinning jet will be directed towards to the pin electrode, where the desired deposition position is located. No delayed zone will appear as shown in Fig. 9(b). Hence, the proposed design would have better performance in terms of deposition accuracy and fabrication of two-dimensional complex patterns with small feature size. For example, a character “C” shape of roughly 300 μm were fabricated using both the conventional and our proposed setups. As shown in Fig. 10(a), the collected fiber patterns are severely distorted using the conventional setup due to the continuous directional changes. While as shown in Fig. 10(b), the fibers are collected according to the intended trajectory.

3.5. Fabrication of complex patterns

The deposition of complex patterns with various geometric characteristics were successfully fabricated in this section to demonstrate the capability of proposed near-field electrospinning setup utilizing the electric field manipulation with a stationary collector. Direct writing of a pair of four-characters “CUHK” with different translation speeds of the bottom pin electrode was tested. The results are shown in Fig. 11. The translation speed was set at 6 mm/s for the results in Fig. 11(a) and 8 mm/s for those in Fig. 11(b). Both cases with different translation speeds have shown good outline geometry of intended patterns. When the translation speed was small (Fig. 11(a)), the bulking effect occurred as expected. When the translation speed was set close to the critical velocity, smooth single fiber patterns could be collected as shown in Fig. 11(b), which directly followed the motion trajectory of the bottom pin electrode. The results have shown that the fiber deposition can be effectively controlled utilizing the electric field distribution rather than the mechanical motion of a collector.

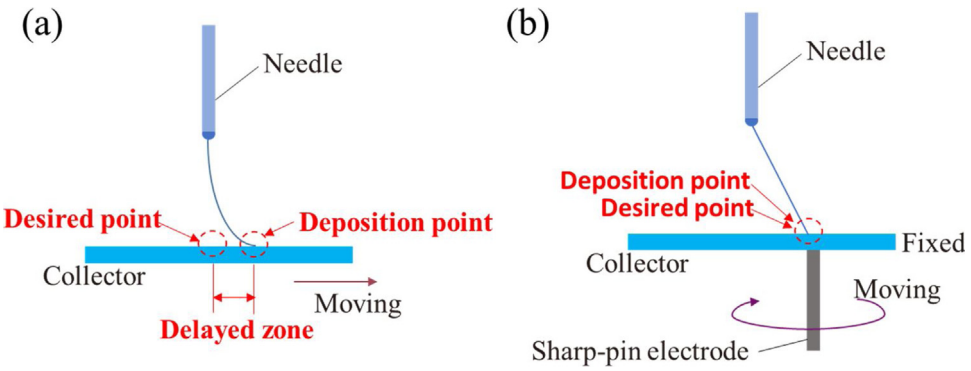

Fig. 9. Comparison between (a) a conventional setup and (b) our proposed setup with different collection mechanisms.

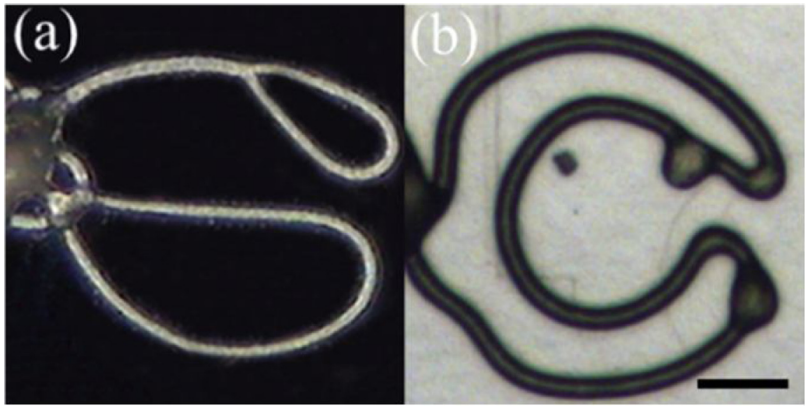

Fig. 10. Fabricated fiber patterns of character "C" with different collection mechanisms: (a) conventional setup and (b) our proposed setup. (The scale bar is 100 μm.).

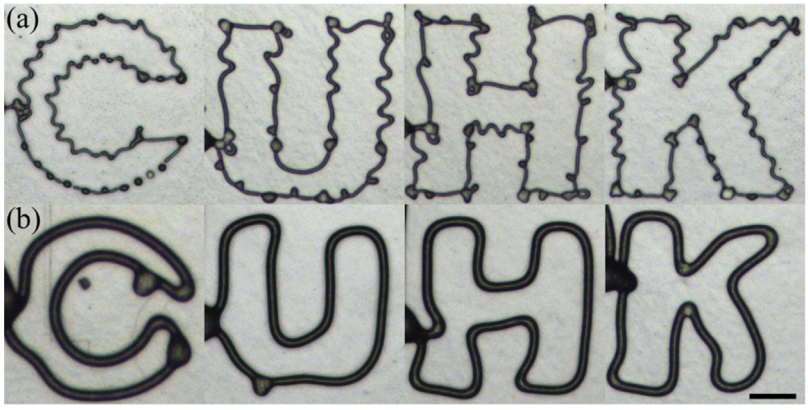

Fig. 11. Experimental results of fabricated fiber patterns in four-characters "CUHK" with different translation speed: (a) 6 mm/s and (b) 8 mm/s. (The scale bar is 100 μm.).

4. Conclusions

In this paper, an innovative design by adding a moving sharp-pin electrode beneath a stationary collector is proposed, aiming to control a near-field electrospinning jet by electric field manipulation. The deposition accuracy is much improved compared with the conventional setup which utilizes a plane bottom electrode as a movable collector. The effects of electric field focusing and jet trajectory guiding are simulated and verified. Various parameters (voltage, translation speed, and collection mechanism) are experimentally analyzed to study their effects on the fiber deposition control. The collection mechanism between a conventional near-field electrospinning setup and our proposed setup is compared to demonstrate the advantages of the proposed setup for better fiber deposition control. Owing to the fact that no delayed zone will appear in the proposed setup, it has better performance in terms of deposition accuracy and fabrication of two-dimensional complex patterns. Two-dimensional fiber patterns with various geometrical characteristics and small feature size have been successfully fabricated. The collected patterns are in good agreement with the moving trajectory of the pin electrode.

Acknowledgements

This work has been supported by the Shun Hing Institute of Advanced Engineering, The Chinese University of Hong Kong, #BME-p6-16; and Research Grants Council of Hong Kong, #ECS 24201816.

References

[1] Ki CS, Gang EH, Um IC, Park YH. Nanofibrous membrane of wool keratose/silk fibroin blend for heavy metal ion adsorption. J Membr Sci 2007;302:20–6.
[2] Gibson P, Schreuder-Gibson H, Rivin D. Transport properties of porous membranes based on electrospun nanofibers. Coll Surf A 2001;187:469–81.
[3] Khil MS, Cha DI, Kim HY, Kim IS, Bhattarai N. Electrospun nanofibrous polyurethane membrane as wound dressing. J Biomed Mater Res B Appl Biomater 2003;67:675–9.
[4] Li WJ, Laurencin CT, Caterson EJ, Tuan RS, Ko FK. Electrospun nanofibrous structure: a novel scaffold for tissue engineering. J Biomed Mater Res A 2002;60:613–21.
[5] Zeng J, Xu X, Chen X, Liang Q, Bian X, Yang L, et al. Biodegradable electrospun fibers for drug delivery. J Controll Release 2003;92:227–31.
[6] Choi SW, Jo SM, Lee WS, Kim YR. An electrospun poly (vinylidene fluoride) nanofibrous membrane and its battery applications. Adv Mater 2003;15:2027–32.
[7] Liu H, Kameoka J, Czaplewski DA, Craighead H. Polymeric nanowire chemical sensor. Nano Lett 2004;4:671–5.
[8] Hahm J, Lieber CM. Direct ultrasensitive electrical detection of DNA and DNA sequence variations using nanowire nanosensors. Nano Lett 2004;4:51–4.
[9] A. Formhals, Process and apparatus for preparing artificial threads, U.S. Patent 1975504, 1934.
[10] A. Formhals, Method and apparatus for spinning, U.S. Patent 2349950, 1939.
[11] A. Formhals, Artificial thread and method of producing same, U.S. Patent 2187306, 1940.
[12] Reneker DH, Chun I. Nanometre diameter fibres of polymer, produced by electrospinning. Nanotechnology 1996;7:216.
[13] Deitzel J, Kleinmeyer J, Hirvonen J, Tan NB. Controlled deposition of electrospun poly (ethylene oxide) fibers. Polymer 2001;42:8163–70.
[14] Reneker DH, Yarin AL, Fong H, Koombhongse S. Bending instability of electrically charged liquid jets of polymer solutions in electrospinning. J Appl Phys 2000;87:4531–47.
[15] Li D, Wang Y, Xia Y. Electrospinning nanofibers as uniaxially aligned arrays and layer-by-layer stacked films. Adv Mater 2004;16:361–6.
[16] Carnell LS, Siochi EJ, Holloway NM, Stephens RM, Rhim C, Niklason LE, et al. Aligned mats from electrospun single fibers. Macromolecules 2008;41:5345–9.
[17] Lee J, Lee SY, Jang J, Jeong YH, Cho D-W. Fabrication of patterned nanofibrous mats using direct-write electrospinning. Langmuir 2012;28:7267–75.
[18] Sun D, Chang C, Li S, Lin L. Near-field electrospinning. Nano Lett 2006;6:839–42.
[19] Hellmann C, Belardi J, Dersch R, Greiner A, Wendorff J, Bahnmueller S. High precision deposition electrospinning of nanofibers and nanofiber nonwovens. Polymer 2009;50:1197–205.
[20] Chang C, Limkrailassiri K, Lin L. Continuous near-field electrospinning for large area deposition of orderly nanofiber patterns. Appl Phys Lett 2008;93:123111.
[21] Bisht G, Nesterenko S, Kulinsky L, Madou M. A computer-controlled near-field electrospinning setup and its graphic user interface for precision patterning of functional nanofibers on 2D and 3D substrates. J Lab Autom 2012;17:302–8.
[22] Wei C, Dong J. Direct fabrication of high-resolution three-dimensional polymeric scaffolds using electrohydrodynamic hot jet plotting. J Micromech Microeng 2013;23:025017.
[23] Brown TD, Dalton PD, Hutmacher DW. Direct writing by way of melt electrospinning. Adv Mater 2011;23:5651–7.
[24] Bellan LM, Craighead H. Control of an electrospinning jet using electric focusing and jet-steering fields. J Vacuum Sci Technol B 2006;24:3179–83.
[25] Carnell LS, Siochi EJ, Wincheski RA, Holloway NM, Clark RL. Electric field effects on fiber alignment using an auxiliary electrode during electrospinning. Scr Mater 2009;60:359–61.